ISTITUTO NAZIONALE DI FISICA NUCLEARE

Sezione di Milano

INFN/TC-89/12

25 Ottobre 1989

A. Bosotti, M. Di Giacomo, A. Gallo, C. Pagani:

ANALOG CONTROL LOOPS FOR THE MILAN K800 CYCLOTRON RF SYSTEM

Servizio Documentazione
dei Laboratori Nazionali di Frascati

ISTITUTO NAZIONALE DI FISICA NUCLEARE
Sezione di Milano

INFN/TC-89/12
25 Ottobre 1989

ANALOG CONTROL LOOPS FOR THE MILAN K800 CYCLOTRON RF SYSTEM

A. Bosotti+, M. Di Giacomo*, A. Gallo° and C. Pagani+
+Istituto Nazionale di Fisica Nucleare and Universita' di Milano, Milano, Italy.
*Istituto Nazionale di Fisica Nucleare - L.N.S., Catania, Italy.
°Istituto Nazionale di Fisica Nucleare - L.N.F., Frascati (Roma), Italy.

ABSTRACT

In this paper the design criteria and the main features of the two analog feedback loops which are used to control the phase and the amplitude stability of the Milan Superconducting Cyclotron accelerating voltage are described, together with the resonator fine tuning system.

The experimental results, obtained during the full power tests of the first RF cavity, are also presented. A phase stability better than $\pm$ 0.2° and an amplitude modulation noise below $5 \cdot 10^{-5}$ at 100 kV peak dee voltage were routinely achieved all over the frequency range (15÷48 MHz).

1.- INTRODUCTION

The accelerating system of the Milan Superconducting Cyclotron consists of three dees, placed inside the valleys, the cyclotron being a K800, compact, three sectors machine. Each dee is the high voltage inner part of a coaxial resonator which consists of two $\lambda/4$ half cavities, tied together at the center and symmetrically placed with respect to the accelerator median plane [1,2].

The cyclotron design calls for a peak dee voltage of 100 kV in the

injection and extraction regions, the three dee voltages being in phase or ± 120° out of phase depending on the harmonic in use [3]. The design phase stability is ± 0.2° for an amplitude modulation noise of $5 \cdot 10^{-5}$, in order to introduce a minor contribution to the beam energy spread, which is assumed to be of the order of 10^{-3}. Because both the amplitude and the phase of the accelerating voltage have slow and fast variations above these limits, two high d.c. gain feedback loops are needed to reach the design goals.

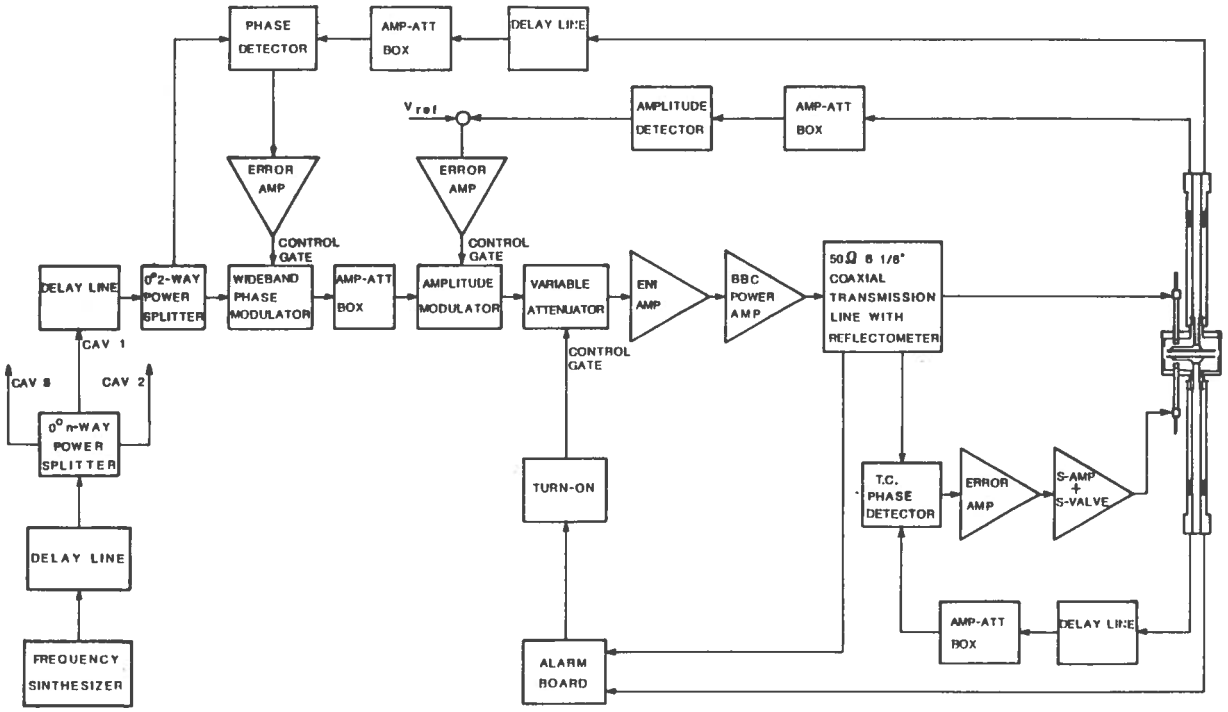

FIG. 1 - RF Control Electronics block diagram.

The accelerating voltage is amplitude and phase modulated by the 50 Hz and its harmonics (in particular 100 and 300 Hz) coming from the ripple of the RF amplifier power supplies. Nevertheless, because the maximum modulation noise which can be accepted, with respect to the carrier, is lower for amplitude, the amplitude loop gain must be higher.

The phase is strongly affected by the cavity thermal drifts, due to Joule effect. In fact a temperature change leads to a cavity geometry variation and this means a detuning of the resonator. Due to the high Q of the resonator, a small detuning leads to a considerable phase shift. A similar effect, but much smaller, is related to the thermal detuning of the power amplifier tank circuits, which have a two orders of magnitude lower Q

factor.

The last cause of the amplitude and phase noise is related to the small mechanical vibrations, of the cavity and tank circuit components, induced by the water and air cooling systems and by the moving piston of a special refrigerator cryopump assembled inside the accelerating structure [4].

As a synthesis, we have two different kinds of phase and amplitude variations: a periodic one, due to the amplifier power supplies and the mechanical vibrations, and an aperiodic one, slower than the former, principally determined by the cavity thermal drifts. We control all these modulations using two feedback loops, based on amplitude and phase modulators, while a trimming capacitor, faced to the dee (and inserted in another phase loop), controls each cavity geometry change, to maintain the phase shift well inside the phase modulator dynamic range. The trimming capacitor movement causes a slow modulation which is well corrected by the two stabilization loops.

A blocks diagram of the accelerating voltage control electronics is presented in Fig. 1

2.- CAVITY RESPONSE TO A MODULATED SIGNAL

To correctly design the feedback systems we start to consider the response of a high Q resonant circuit to a modulated signal.

Limiting the analysis to our case, in which the cavity resonator is capacitively coupled, close to the resonant frequency the transfer function for an input signal is given by:

$$T(j\omega) = R(j\omega)\, e^{j\Theta(j\omega)} = - \frac{\omega^2 R_{eq} C_c / \omega_o Q}{1-\omega^2/\omega_o{}^2 + j\omega/\omega_o Q} \qquad (1)$$

where: R_{eq} is the cavity shunt resistance, C_c is the coupling capacitance, ω_o is the resonance frequency of the system (in the 15÷48 MHz range) and Q its quality factor (of the order of few 10^3).

Equation 1) easily leads to the following two:

$$R(j\omega) = \frac{\omega^2 R_{eq} C_c / \omega_o Q}{\sqrt{[1-(\omega/\omega_o)^2]^2 + (\omega/\omega_o Q)^2}} = R_{max} \frac{(\omega/\omega_o)^2}{\sqrt{Q^2[1-(\omega/\omega_o)^2]^2 + (\omega/\omega_o)^2}} \qquad (2)$$

$$\Theta(j\omega) = \pi/2 + \arctan\left[Q\,\frac{1-(\omega/\omega_o)^2}{\omega/\omega_o}\right] \qquad (3)$$

where R_{max} is the maximum value of the transfer function module.

Let us consider waveforms of frequencies $\omega_o+\omega'$, where ω'/ω_o is less than 10^{-3} (like for the spectra of our typical signals); then Eqs. 2) and 3) can be well approximated by the following two:

$$R(\omega_o+\omega') \simeq \frac{R_{max}}{\sqrt{1+(\omega'/\omega_k)^2}} \qquad (2')$$

$$\Theta(\omega_o+\omega') \simeq \pi/2 - \arctan(\omega'/\omega_k) \qquad (3')$$

where $\omega_k \equiv \omega_o/2Q$ gives the resonant transfer function bandwidth, which in our system is of the order of few kHz.

The accuracy of Eqs. 2') and 3') is of the order of 1% and it is considered adequate for the following analysis.

Particularly, let us consider first an AM signal of the following form:

$$v_i(t) = A\,[1 + m\cos(\omega_m t)]\cos[(\omega_o+\Delta\omega)t] \qquad (4)$$

having a carrier frequency $\omega_c \equiv \omega_o+\Delta\omega$ close to the resonance value ω_o. In particular, because of the fine tuning system operation, we have: $\Delta\omega/\omega_k << 1$.

To find the response $v_o(t)$ to the signal given by Eq. 4) we evaluate the response to each input spectral line, expanding to the first order the functions of the $\Delta\omega/\omega_k$ variable. Thus we obtain:

$$v_o(t) \simeq A\,R_{max}\left[1+\frac{m}{\sqrt{1+(\omega_m/\omega_k)^2}}\cos\left(\omega_m t-\arctan(\omega_m/\omega_k)\right)\right]\cos\left[\omega_c t+\pi/2-\Delta\omega/\omega_k+\right.$$

$$\left.-\Delta\omega/\omega_k\,\frac{m}{1+(\omega_m/\omega_k)^2}\cos\left(\omega_m t - 2\arctan(\omega_m/\omega_k)\right)\right] \qquad (5)$$

A very similar result is obtained considering a NBFM input signal (a PM signal with $\beta << 1$ rad.):

$$v_i'(t) = A \cos[(\omega_o+\Delta\omega)t + \beta \sin(\omega_m t)] \qquad (6)$$

which gives the following output signal:

$$v_o'(t) = A\, R_{max} \left[1+(\Delta\omega/\omega_k)\, \frac{\beta}{1+(\omega_m/\omega_k)^2} \sin\left(\omega_m t - 2 \arctan(\omega_m/\omega_k)\right)\right] \cdot$$

$$\cdot \cos\left[\omega_c t+\pi/2 - \Delta\omega/\omega_k + \frac{\beta}{\sqrt{1+(\omega_m/\omega_k)^2}} \sin\left(\omega_m t - \arctan(\omega_m/\omega_k)\right)\right] \qquad (7)$$

Equations 5) and 7) point out that an AM or NBFM signal feeding a resonant circuit produces an output signal both amplitude and phase modulated. Particularly, comparing the input and the output waveforms, we can conclude that a modulating input signal is transformed in two different modulating terms: one "homogeneous" (i.e. of the same kind: AM or PM respectively) and the other "spurious" (i.e. of the other kind). The transformation laws are given, in the Laplace s-domain, respectively by the two following transfer functions:

$$L(s) = \frac{1}{1 + s/\omega_k} \qquad (8)$$

$$H(s) = \pm \frac{\Delta\omega/\omega_k}{(1 + s/\omega_k)^2} \qquad (9)$$

In Eq. 9) the "-" sign refers to an AM input, while the the "+" sign refers to a NBFM input.

Equation 8) states that a resonant circuit behaves, for homogeneous input and output terms, like a low-pass filter (LPF), with a single pole located at the frequency $\omega_k \equiv \omega_o/2Q$. Thus Eq. 8) transfer function must be carefully taken into account for the development of accelerating voltage phase and amplitude stabilization loops.

Equation 9) states that the two different kinds of modulation are intrinsically coupled in a resonator. The coupling transfer function has a double pole at the frequency ω_k and the coupling degree is linearly related to the detuning level.

Few more comments on this topic are included in the last section of this paper.

3.- FINE TUNING SYSTEM

Fine tuning of the resonator is accomplished by means of a trimming capacitor just above the dee. The movable head is actuated by a hydraulic piston servo with a stroke of 50 mm. The position of the trimming capacitor can be set either manually or automatically. Particularly, the capacitor can be manually moved from the computer control console, while in the automatic mode the system is included in a feedback loop specified below.

As we told before the cavity geometry changes due to Joule effect during power operation, and so the resonance frequency changes too. Because of the high cavity Q, a small detuning leads to a consistent phase shift, according to the following equation:

$$\Delta f = \frac{f_o}{2Q} \Delta\phi \qquad (10)$$

where $\Delta\phi$ is the phase shift due to a detuning Δf from the resonance frequency f_o. A closed loop geometrical compensation is necessary to keep the detuning well inside the dynamic range of the amplitude and phase loops.

The fine tuning system detects any resonance frequency drift looking at the phase angle between the forward wave and the dee voltage. When the resonator is properly tuned and matched to the transmission line, the phase angle at the phase detector input is set to zero. The block diagram of the fine tuning system is shown in Fig. 2.

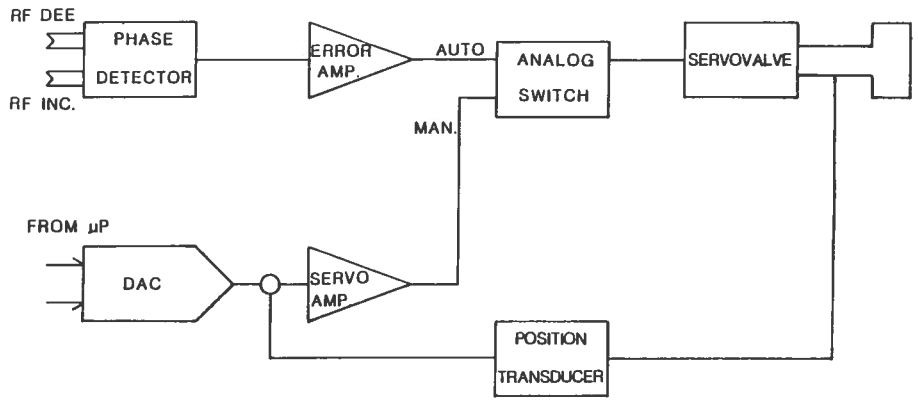

FIG. 2 - Fine tuning system block diagram

Referring to the block diagram, the hydraulic position servo is mainly composed by an hydraulic linear actuator servovalve and a position transducer.

We want to point out that the system must have a very high loop gain at very low frequencies, also if the piston behaves as an integrator and the servovalve has a low frequency pole. In fact the transfer functions of the servovalve $T_v(s)$ and of the piston $T_p(s)$ are given respectively by:

$$T_v(s) = \frac{W}{I} = \frac{K_1}{1 + s\tau_v} \qquad (11)$$

$$T_p(s) = \frac{X}{W} = \frac{K_2}{As} \qquad (12)$$

where: W is the oil flow; I is the servovalve control current and τ_v its time constant; A is the piston area and X its head position.

The phase detector, which is the most critical electronic device of the fine tuning system (Fig. 3), has been designed around a 3 dB quadrature hybrid (Merrimac QHS-6-42). When the two input signals (applied at port 1 and 4) are in phase, independently from their reciprocal amplitudes, the output signals (at port 2 and 3) have the same amplitude, while if the two input signals are out of phase the output signal amplitudes are different.

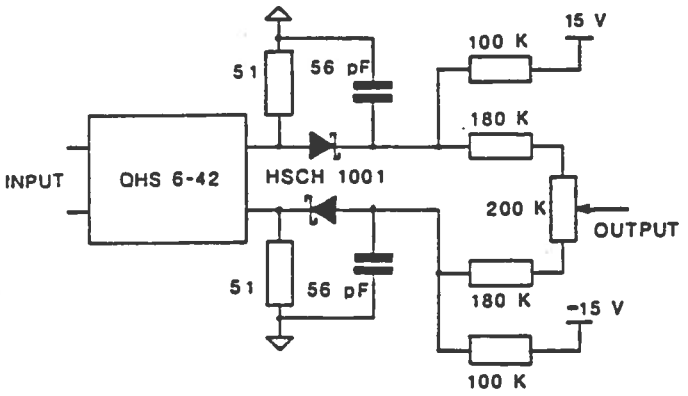

FIG. 3 - Phase detector

Ports 2 and 3 are followed by two biased Schottky diode amplitude detectors. The first one detects the positive peak and the other the negative one. The two demodulated signals feed the terminals of a symmetric (with respect to the sampling point) resistive network. If the two DC signals are of the same amplitude, the sampled voltage is zero; otherwise it is related to the phase difference and has the same sign. The sampled signal is then buffered and sent to the input of the fine tuning system integrator.

The phase detector output voltage $V_{out}(\Delta\phi)$ is given by:

$$V_{out}(\Delta\phi) = \frac{1}{\sqrt{2}} \left[\sqrt{A_1^2+A_4^2+2A_1A_4\sin\Delta\phi} - \sqrt{A_1^2+A_4^2-2A_1A_4\sin\Delta\phi} \right] \qquad (13)$$

where A_1 and A_4 are the RF levels coming in the ports 1 and 4 of the 90° hybrid, while $\Delta\phi$ is the phase angle between them.

4.- AMPLITUDE LOOP

As mentioned above, the amplitude loop must ensure an amplitude modulation noise below $5 \cdot 10^{-5}$. The block diagram is shown in Fig. 4.

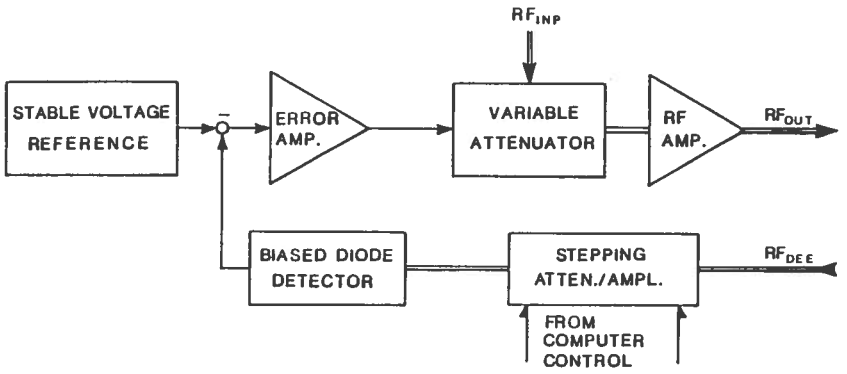

FIG. 4 - Amplitude loop block diagram

The amplitude modulator is based on a double balanced mixer variable attenuator (MCL ZAS 3), driven by a high gain error amplifier. The error is the difference between a high stability voltage reference (AD 584 LH), which controls the dee voltage, and a demodulated sample of the dee voltage, picked-up by a loop placed on one of the short circuit plates of the resonator [2].

We developed a two-stage error amplifier having a particular transfer function to ensure a high loop gain together with an adequate stability phase margin (≃45°). Each stage is based on the well know LM741 operational amplifier and the resulting transfer function $T_1(s)$ is the following:

$$T_1(s) = K \frac{1 + s\tau}{s\tau'} \qquad (14)$$

The rationale of the choice of such an error amplifier is that it ensures a very high dc gain, controlled by the second stage, and it places a zero at a proper frequency ($\simeq$ 1.5 kHz), lower than the frequency of the cavity pole, in order to control the error bandwidth.

Finally, due to the relatively low Q (< 100) of the tank circuits of the power amplifier, its pole does not affect the loop stability, having a frequency of some hundred of kHz.

An amplitude detector has been especially designed to reach acceptable performances, with respect to our specs. Particularly, its main characteristics are the following:

- good linearity of the detection characteristic;
- insensitivity to the phase modulations, in order to minimize the contribution to the amplitude and phase loops coupling;
- long term stability, because transfer characteristic drift would be considered like dee voltage variation;
- wide bandwidth: in particular the devices must cover the frequency range 15÷48 MHz.

The amplitude loop amplitude detector is a peak envelope detector based on a silicon hot carrier diode (MBD 501). The diode bias current is optimized to reach a good compromise between residual ripple level and "failure to follow distortion" threshold.

The optimized Bode plots of the amplitude feedback loop gain, at two different frequencies, are presented in Fig. 5, for a phase margin of 45°.

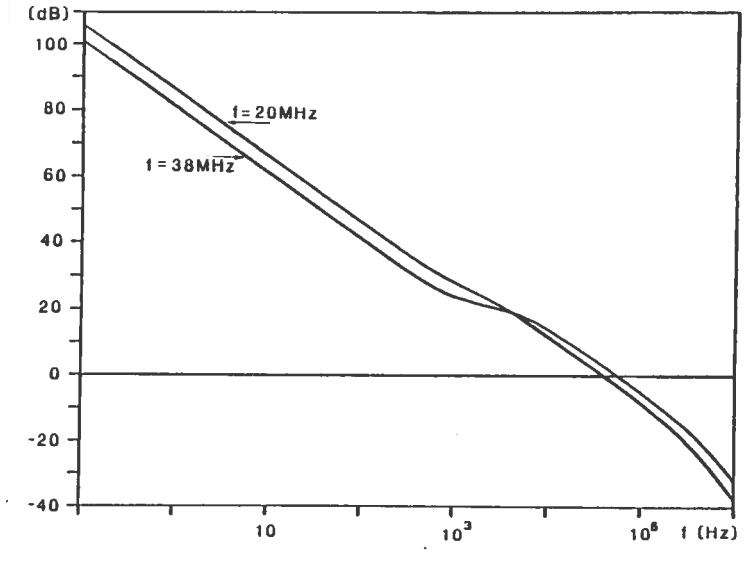

FIG. 5 - Bode plot of the amplitude feedback loop gain (see text for details).

In the same figure the displacement of the cavity and power amplifier poles, as a function of frequency, can also be seen. Inside the operational frequency range, the loop gain plots are limited by the two presented curves.

The overall behavior of this stabilization system can be described, in the Laplace s-domain, by the use of a proper mathematical model of the loop, leading to the following transfer function, which express the closed to open loop amplitude noise ratio:

$$G_a(s) = \frac{1}{1 + V_{ref} \frac{d\alpha}{dV_c}(V_c)\, L(s)\, T_1(s)} \qquad (15)$$

In Eq. 15) V_{ref} is the voltage reference level, $\alpha(V_c)$ is the attenuation versus working point function of the variable attenuator, $T_1(s)$ is the error amplifier transfer function (given by Eq. 14), and L(s) is the LPF transfer function related to the cavity and power amplifier resonant behavior (Eq. 8).

The amplitude loop working point must be chosen in such a way that the loop is stable for each frequency and amplitude of the accelerating RF voltage, together with the maximum loop gain. Nevertheless either the loop components or the pick-ups (used to take samples of the dee voltage) are strongly influenced by the signal frequency and amplitude. In particular we have that the coupling between the inductive loops and the field increases with the frequency, and so we have different input voltages to the amplitude detector and the variable attenuator that lead to a change in the loop gain.

So that, to have an optimum loop gain in spite of the working parameters, we developed a stepping attenuator/amplifier in order to keep the loop gain independent from the amplitude and the frequency of the sampled signals. This component is a computer controlled device designed to control the amplitude of the RF power in a range of $\pm$ 20 dB with 1 dB step.

As an example two spectra (with and without feedback) of the measured amplitude noise are shown in Fig. 6, for a typical setting of the cavity operation parameters. Comparing the spectra with closed or open loop, it is apparent that the loop gain has the frequency dependence presented in Fig. 5, the residual noise being below the design values.

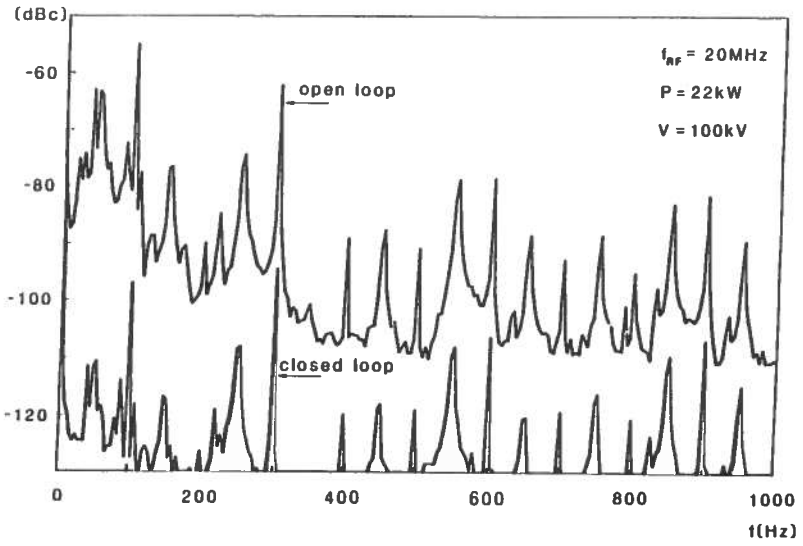

FIG. 6 - Measured amplitude noise spectra, with and without feedback, for a typical setting of the cavity operation parameters.

5.- PHASE LOOP

Like for the amplitude, a phase loop is used to reduce the phase modulation below ± 0.2°. Its block diagram is presented in Fig. 7.

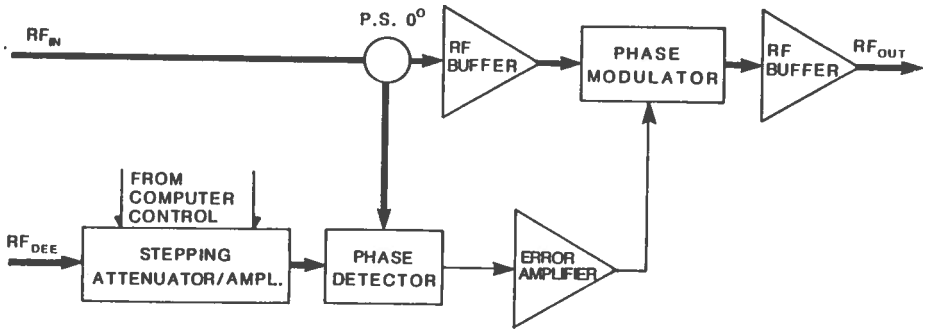

FIG. 7 - Block diagram of the phase stabilization loop.

The phase modulator performs a vector modulation acting on the two orthogonal components of the input RF signal, obtained by means of a 3 dB quadrature hybrid; its block diagram is presented in Fig. 8.

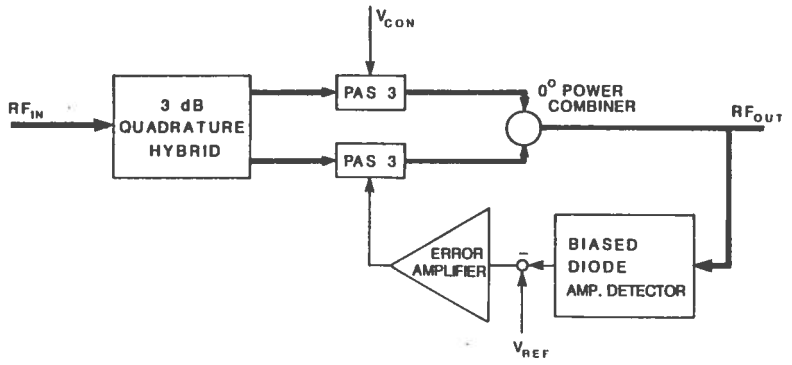

FIG. 8 - Phase modulator block diagram.

In order to ensure a very low coupling between the amplitude and the phase loops, the phase modulator is designed to have a very small residual amplitude modulation. This task is mainly accomplished by the phase modulator amplitude loop and by the RF buffers (see Fig. 8), used for a proper impedance matching.

The phase detector is based on an analog multiplier (XR 2208). The output signal V_f is given by:

$$V_f = K_o \cos\Delta\phi \qquad (16)$$

where: $\Delta\phi$ is the phase difference between the two input signals and K_o is a parameter that depends on the amplitude and the frequency of the input signals, one of which is the phase reference signal, while the other is a sample of the dee voltage.

Looking at Fig. 7, Eq. 16) shows that the phase modulator must be able to set a phase difference of $\simeq 90°$ between the two input signals of the phase detector, in order to prevent the high gain error amplifier saturation. Furthermore, to give a constant contribution to the loop gain, the input signal levels must be kept constant, in spite of the setting of the accelerating voltage amplitude and frequency.

A stepping attenuator/amplifier, similar to that described for the amplitude loop, is used to keep constant the signal amplitude, and a programmable delay line is used to control the phase modulator operating point while it maintain the 90° phase condition.

This last device is a modular six bits computer controlled stepping line (1 ns step for 63 ns maximum delay) together with a continuously tunable line, for fine adjustment in between two adjacent steps. A picture of this

device connected to its control circuit is shown in Fig. 9.

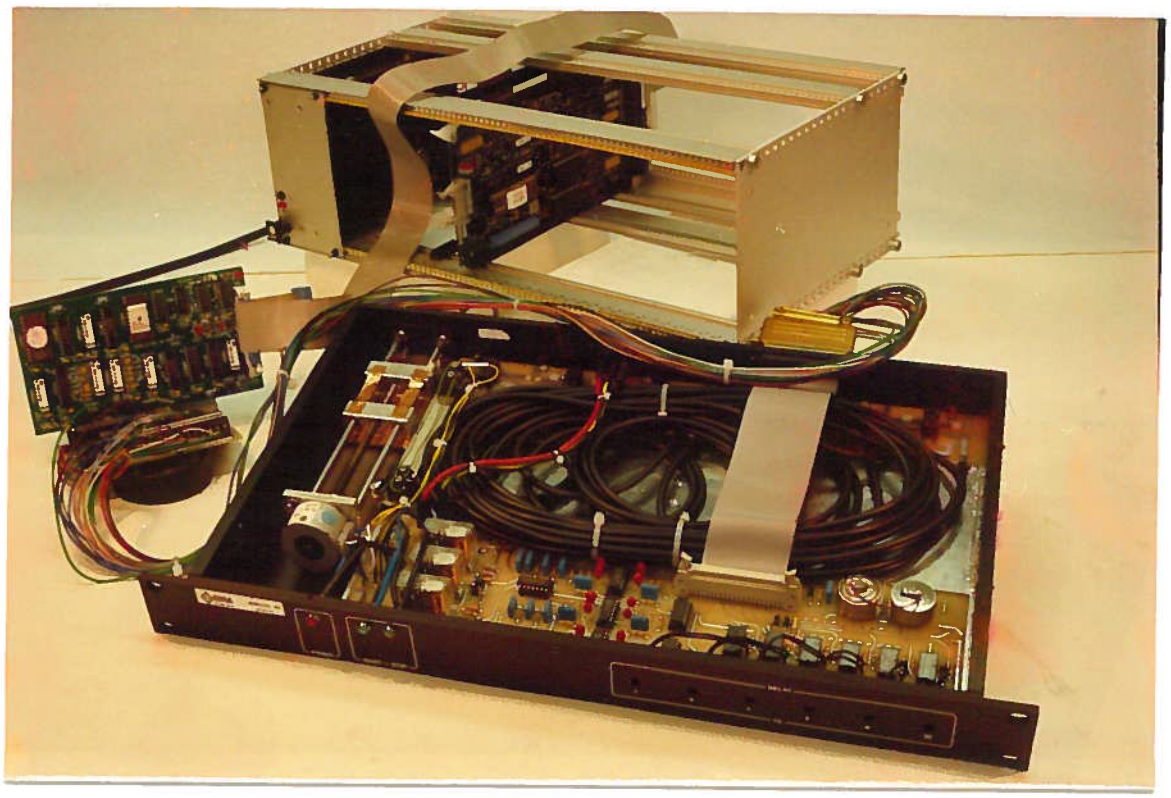

FIG. 9 - Computer controlled delay line phase shifter.

Because the problem of the system stability is very similar to that of the amplitude loop, the error amplifier is analogous to that used for the amplitude loop.

With the aid of a mathematical model, we can describe the stabilization capability of such a system by mean of a transfer function $G_p(s)$, giving the closed to open loop phase noise ratio in the Laplace s-domain:

$$G_p(s) = \frac{1}{1 - \frac{1}{V_c}\frac{dV_d}{d\Delta\Phi}(\Delta\Phi_o)\, L(s)\, \Theta(s)\, T_2(s)} \qquad (17)$$

where: V_c is the phase modulator working point, $V_d(\Delta\Phi)$ is the analytical expression of the phase detector characteristic, $\Theta(s)$ is the phase versus control waveform transfer function of the modulator, $L(s)$ is still the LPF transfer function (Eq. 8), and $T_2(s)$ is the error amplifier transfer function (refer to Eq. 14).

6.- INTERACTION BETWEEN LOOPS

The stabilization loops described above interact in a number of ways.

First the fine tuning system follows its equilibrium position with damped oscillation that cause slow and aperiodical phase and, at the second order, amplitude modulation. Such modulations are a further load for both phase and amplitude stabilization loops, but each loop has a high d.c. gain error amplifier and so this additional noise is well controlled.

Besides the phase and amplitude loops have reciprocal influences, i.e. the amplitude loop gives a phase modulation and vice versa the phase loop.

We point out that to have a functional decoupling between the loops we must employ at least one detector (amplitude or phase) having a very high insensitivity to the other kind of modulation. In our system, this is the case for the amplitude detector, which, being a polarized negative envelope peak detector, performs a very high rejection of the phase noise. Thus the transfer functions of the two stabilization loops are practically independent and the mutual interaction is limited to a reciprocal increase of the noise levels.

We have two different contributions to this kind of interaction:

- An indirect and intrinsical contribution, given by the mixing phenomenon described above (Eq. 9) and related to the generation of spurious modulation in resonant detuned circuits. The only way to limit this phenomenon is to employ an efficient fine tuning system, having a coupling factor $\Delta\omega/\omega_k$ always much smaller than 0.1.
- A direct contribution, given by the phase and amplitude modulators which introduce, beside the desired modulation, a certain amount of noise on the not controlled quantity (i.e. the amplitude for the phase modulator and vice versa).

This contribution is strictly related to the non-ideality of the employed devices.

Since the design level of the amplitude stability ($5 \cdot 10^{-5}$ ~ 92 dBc) is much more critical than that of the phase stability ($\pm$ 0.2° ~ 55 dBc), we employ an amplitude stabilized phase modulator to minimize the direct production of amplitude noise in the system, the internal amplitude loop of the phase modulator having a loop gain of 30 dB. On the contrary, we do not need phase stabilization for the amplitude modulator.

7.- CONCLUSIONS

The electronic systems presented in this paper are the final version of the prototypes extensively tested since 1985 [2]. Because of the significant delay of few major components of the Milan Superconducting Cyclotron [6], these systems, together with all the others circuits of the RF control [5], have been redesigned, in order to increase reliability and simplify the maintenance procedures. Moreover, all the settings, needed to operate the cyclotron RF system at a certain frequency and dee voltages, are now fully computer assisted [7].

The picture of Fig. 10 shows a typical rack with few different electronic sub-systems assembled. Each sub-system has a separate cabinet with a mimic diagram on the front panel, including test points and status signals. All the input/output cables, connecting the cabinets, are in the rear panels.

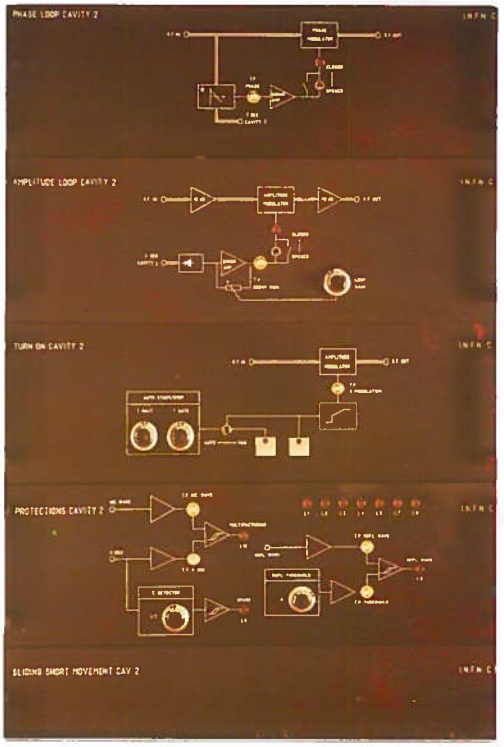

FIG. 10 - Typical RF rack.

REFERENCES

[1] - C. Pagani, Proc. X Int. Conf. on Cyclotrons, East Lansing 1984, IEEE cat. N. 84CH 1966-3, p. 305.

[2] - C. Pagani et al., Proc. XI Int. Conf. on Cyclotr., Tokyo 86, IONICS Pub., p. 271.

[3] - A. Acerbi et al., Proc. X Int. Conf. on Cyclotr., East Lansing 1984, IEEE cat. 84CH 1966-3, p. 251.

[4] - P. Michelato, C. Pagani & A. Giussani, Proc. 1st European Particle Accelerator Conference, Roma, June 1988, World Scientific Pub., pag. 1278.

[5] - A. Bosotti, W. Lovati & C. Pagani, Report INFN/TC-86/6, 1986.

[6] - A. Acerbi et al., Proc. 1st European Particle Accelerator Conference, Roma, June 1988, World Scientific Pub. pag. 323.

[7] - A. Bosotti et al., Proc. 1st European Particle Accelerator Conference, Roma, June 1988, World Scientific Pub. pag. 1306.